Hierarchical globally coupled systems

Sudeshna Sinha
The Institute of Mathematical Sciences, CIT Campus, Madras 600 113, India

Gabriel Pérez
Departamento de Física Aplicada, CINVESTAV del IPN, Unidad Mérida, Apartado Postal 73 ''Cordemex,'' 97310 Mérida, Yucatán, Mexico

Hilda A. Cerdeira
International Centre for Theoretical Physics, P.O. Box 586, Trieste 34100, Italy

(Received 26 April 1997; revised manuscript received 9 June 1997)

We have constructed prototype models of globally coupled systems on lattices with space-time hierarchy. In our models fully chaotic dynamical elements at a certain level in the hierarchy are coupled to the levels immediately above and below in the hierarchy through their mean fields. We report the wealth of spatiotemporal phenomena our models yield and give detailed bifurcation diagrams in coupling parameter, ϵ, space $(0 \leqslant \epsilon \leqslant 1)$. We find that over a large range of strong coupling $(0.5 < \epsilon \leqslant 1)$ our models quickly evolve into a spatiotemporal fixed point. We analyze the stability of this phase. For moderate coupling $0.15 < \epsilon < 0.5$, we have spatial inhomogeneity and temporal regularity, marked by the presence of, either exact 2^k, $k = 1,2 \ldots$ cycles, or noisy bands (characterized by δ spikes on a noisy background in the power spectra). An interesting feature of this phase is the presence of several coexisting attractors, with fractal basin boundaries. For small coupling $(\epsilon \sim 0.1)$ we show that our system, while temporally chaotic and spatially nonhomogeneous, develops certain broad periodicities in their mean field, especially at finer scales. In addition, if one looks at the fluctuation of the mean field at various levels in the hierarchy in this phase, one finds that the mean square deviation does not decrease as $1/N$ with N, where N is the number of elements at a particular level. Instead it displays marked nonstatistical behavior with the deviations saturating (or even increasing) for high N. [S1063-651X(98)09704-9]

PACS number(s): 05.45.+b

I. INTRODUCTION

Global coupling in dynamical systems yields a host of very novel features. This class of systems is of considerable interest in modeling phenomena as diverse as Josephson junction arrays, multimode lasers, vortex dynamics, and even evolutionary dynamics, biological information processing and neurodynamics. More generally global coupling appears as a result of a mean field approach to the dynamics of distributed systems. The ubiquity of globally coupled phenomena has thus made it a focus of sustained research activity [1–10].

Now a wide range of phenomena, from turbulence to earthquakes, involve a *hierarchy of spatial and temporal scales*. Dynamics occurring on spatially hierarchical media are encountered in many physical processes. For instance, it has been a tenet of the classical view of forebrain organization that perceptual processing is performed via hierarchically organized cortical components. This has important implications for memorized data structures and has practical application in large data storage and retrieval capacity [11]. Another well established example is fractal reaction kinetics, i.e., diffusion controlled reactions with geometrical constraints, as found in heterogeneous kinetics. These can be described by reactions on fractal domains, and find practical applications in reactions in pores of membranes, exciton trapping in molecular aggregates, exciton fusion in composite materials, and charge recombination in clouds and colloids [12]. Furthermore, there are also physical situations where both the temporal and the spatial scales are hierarchical. One important example of this is earthquake dynamics. Earthquakes arise from processes in the lithosphere, which are well characterized by hierarchical discreteness of structure and dynamical time scales [13]. Basically the lithosphere presents a hierarchy of volumes or blocks that move relative to each other. The largest blocks are the tectonic plates $(\sim 10^4$ km). They are divided into smaller blocks, like shields or mountains. After 15–20 divisions we come to grains of rock of mm scale (if not less). The relative movement of the various blocks result in seismic activity. These movements occur on a hierarchy of time scales as well, ranging from ~ 1 to 10 min (elastic shocks), days to months (foreshocks and aftershocks) to 100–500 years (movement of plates). Therefore geophysical processes are strongly nonlinear processes well described by space-time hierarchy.

It is of relevance then to investigate global coupling embedded in a hierarchical space-time structure. The extensive studies on globally coupled maps [1–10], so far, have invariably been defined on regular underlying lattices. (The only examples of attempts to put coupled maps on nonuniform lattices have been maps with *local* diffusive coupling on spatially hierarchical lattices, such as Sierpinski gaskets [14] and Cayley trees [15].) Here we will incorporate *global* coupling on a lattice that has a hierarchical structure in (i) space; and in (ii) both space and time.

Thus, in our prototype model of hierarchical arrays of

globally coupled maps, we bring together two separate concepts: (1) Global coupling, which has successfully captured the essence of a variety of complex spatiotemporal behavior with high connectivity, and (2) hierarchical lattices, which arise as a natural description for phenomena occurring on a range of length and time scales. Our study, we then hope, will allow one to gain insight into a previously unexplored range of spatiotemporal phenomena.

II. MODEL

As mentioned before, in contrast to the widely discussed globally coupled maps, we now incorporate global coupling on a hierarchical lattice. We consider two cases: model I, with hierarchical structure in space (relevant, for instance, in neuronal activity) and model II, which is hierarchical in both space and time (relevant, for example, for geophysical processes such as earthquakes). In our models, space is discrete, time is discrete, and the state variable, which in physical systems could denote macroscopic quantities such as energy, temperature, pressure, fluid velocity or chemical concentration, is continuous. The elementary building block of our hierarchical system is the logistic map, which has widespread relevance as a prototype of chaos:

$$x_\tau = f(x_\tau) = 1 - a x_\tau^2, \quad -1 \leqslant x \leqslant 1, \quad 0 \leqslant a \leqslant 2. \tag{1}$$

Here $\tau = 0,1,2,\ldots$ denotes the discrete time, x is the dynamical variable, and a the control parameter. In our simulations we choose $a=2$, which gives rise to fully chaotic dynamics.

Now we embed this elementary nonlinear dynamical element in a space-time hierarchical lattice. The state variable then will have three indices: space, time, and hierarchy labels. Time, as in the local map, is labeled by τ. Space is labeled by $\mathbf{r} \in \mathbb{Z}^d$, which denotes points on a d-dimensional cubic lattice. Hierarchy is indexed by n, $0 \leqslant n \leqslant L$. We associate the largest n with the smallest (finest) scales. The scales on level n, $n = 0,1,2,\ldots,L$ are given by a typical length scale $\ell^{(n)}$ and a typical time scale $\vartheta^{(n)}$. For simplicity we choose for model I, which has only spatial hierarchy:

$$\ell^{(n)} = 2\ell^{(n+1)}. \tag{2}$$

Spatially, it implies that model I consists of a nested hierarchy of d-dimensional cubes. Level-n cubes contain 2^d level-$(n+1)$ cubes, i.e., level-n contains $(2^n)^d$ sites.

For model II, which has both temporal and spatial hierarchical scales, we have

$$\ell^{(n)} = 2\ell^{(n+1)}, \quad \vartheta^{(n)} = 2\vartheta^{(n+1)}. \tag{3}$$

Spatially, it again implies that this model consists of a nested hierarchy of d-dimensional cubes. In addition, temporally, this means that the value of $x_\tau^n(\mathbf{r})$ is updated only once when $x_\tau^{n+1}(\mathbf{r})$ is updated twice.

The global coupling arises from the interaction of the elements of a level with the mean fields of levels contiguous in the hierarchy. Incorporating this mean-field type interaction term in the dynamics, we obtain the complete dynamical equation for $x_\tau^n(\mathbf{r})$ on level n to be as follows:

For model I:

$$x_{\tau+1}^n(\mathbf{r}) = (1-\epsilon) f(x_\tau^n(\mathbf{r})) + \tfrac{1}{2}\epsilon(h_\tau^{n+1} + h_\tau^{n-1}), \tag{4}$$

where

$$h_\tau^{n-1} = \frac{1}{(2^{n-1})^d} \Sigma_{\mathbf{r}} x_\tau^{n-1}(\mathbf{r}) \tag{5}$$

and

$$h_\tau^{n+1} = \frac{1}{(2^{n+1})^d} \Sigma_{\mathbf{r}} x_\tau^{n+1}(\mathbf{r}). \tag{6}$$

This implies that the elements see an average of the mean field of the finer scale $(n+1)$ and the grosser scale $(n-1)$. The boundary conditions are taken to be as follows: for level $n=L$, $h^{n+1}=0$ and for level $n=0$, $h^{n-1}=0$, for all τ. Also note that dimensionality simply has the effect of altering the number of elements at each level, since coupling is global. The geometry of the $\mathbb{Z}^d$ lattice is not important.

For model II:

$$x_{\tau+1}^n(\mathbf{r}) = \begin{cases} (1-\epsilon) f(x_\tau^n(\mathbf{r})) + \tfrac{1}{2}\epsilon(h_\tau^{n+1} + h_\tau^{n-1}) & \text{if } \tau \equiv 0 \pmod{2^{(L-n)}} \\ x_\tau^n(\mathbf{r}) & \text{otherwise.} \end{cases} \tag{7}$$

where

$$h_\tau^{n-1} = \frac{1}{(2^{n-1})^d} \Sigma_{\mathbf{r}} x_\tau^{n-1}(\mathbf{r}) \tag{8}$$

and

$$h_\tau^{n+1} = \frac{1}{2}\left\{ \frac{1}{(2^{n+1})^d} [\Sigma_{\mathbf{r}} x_\tau^{n+1}(\mathbf{r}) + \Sigma_{\mathbf{r}} x_{\tau-1}^{n+1}(\mathbf{r})] \right\}. \tag{9}$$

This implies that the elements see an average of the mean field of two consecutive time steps of the finer scale, $n+1$ (as it evolves twice as fast as level n), while seeing the same mean field of the grosser scale, $n-1$, for two evolutionary steps (as it evolves half as slowly). (Again, we take for level $n=L$, $h^{n+1}=0$, and for level $n=0$, $h^{n-1}=0$, for all τ).

Further, the above equation for model II means that each time there is a change on level n_0 all levels n with $n > n_0$ will be updated as well. Table I shows the pattern of times τ when the upper line of Eq. (7) applies. In a system with L levels, updates on level n are due at

$$\tau^{(n)}(\sigma) = 2^{L-n}\sigma, \quad \sigma = 0,1,2,\ldots. \tag{10}$$

TABLE I. Times τ at which the upper line of Eq. (7) applies for a system with $L=3$.

$n\backslash\tau$	0	1	2	3	4	5	6	7	8	9	10	11	12	13	14	15
0	x								x							
1	x				x				x				x			
2	x		x		x		x		x		x		x		x	
3	x	x	x	x	x	x	x	x	x	x	x	x	x	x	x	x

We call σ the reduced time on level n. Note that all time series analysis will be with respect to the reduced time σ at each level in the hierarchy, i.e., we will be stroboscopically sampling the state variable at its natural time scale.

Note that in our study we update the levels *asynchronously*, in a certain fixed order, with the sites at each level being updated in parallel (analogous, for instance, to the situation in neuromorphology, where the neurons, neuron groups and functional layers are fully asynchronous). We start from the spatially finest and dynamically fastest level: $n=L$, and go on to the grossest (and slowest) level: $L=0$. At each step we use the *current* values of $x(i)$ to compute the effective mean field [via Eqs. (5) and (6) for model I, and Eqs. (8) and (9) for model II]. On the other hand, one can compute the mean field synchronously (i.e., at the beginning of each time step) and then update sites at all levels simultaneously [16]. See Appendix (A3) for further analysis on the dynamical changes arising from differences in updating rules.

III. RESULTS

For both our models (I and II), we start the numerical simulations with values of $x_0^n(\mathbf{r})$ $(n=0,1,\ldots,L)$ chosen randomly in the interval $[-1,1]$. We record the evolution of the state variables $x_\tau^n(\mathbf{r})$ and the mean field h_τ^n at each level n in the hierarchy, for different values of the coupling parameter ϵ. All results quoted in this paper, unless otherwise stated, are obtained using asynchronous level-by-level updates.

We now present, in the sections below, detailed bifurcation diagrams and descriptions of the different dynamical phases the models yield.

A. Bifurcation diagrams

We first give the bifurcation diagrams of the two models with respect to the entire range of coupling strength ϵ: $0\leqslant\epsilon\leqslant 1$. Figures 1 and 2 give the dynamical phases for model I and model II, respectively. It is clearly evident that for both models two distinct regions emerge: (1) $0.5<\epsilon\leqslant 1.0$ where the system quickly evolves to a spatially synchronous and temporally invariant state for all initial conditions and (2) $0\leqslant\epsilon<0.5$ where we have a variety of behaviors. (At $\epsilon=0.5$ we have marginal stability, marked by very long transients). Note that these bifurcation diagrams have been obtained using only *one* generic initial condition.

Figure 3 (for model I) and Fig. 4 (for model II) depict bifurcation diagrams generated from a large set of random initial conditions. So, while Figs. 1 and 2 basically give the stable attractors for a single typical initial phase point for different values of ϵ, Figs. 3 and 4 give the set of all coexisting attractors to which initial phase points can evolve. For the fixed point attractor all initial conditions are attracted to spatiotemporal invariance. So bifurcation diagrams generated either way are identical. But for the second region, which supports many *coexisting attractors*, the two bifurcation diagrams will necessarily be different, with Figs. 3 and 4

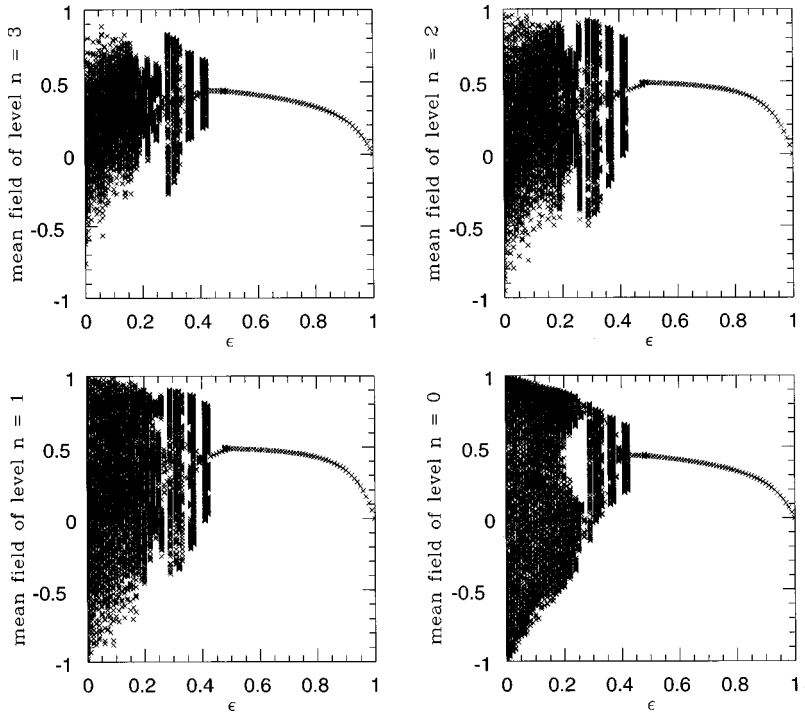

FIG. 1. Bifurcation diagrams for model I, in one dimension (with $L=3$), displaying the various dynamical phases, over the entire range of coupling strength: $0\leqslant\epsilon\leqslant 1$. All four levels in the hierarchy ($n=0,1,2,3$) are depicted. These bifurcation diagrams are generated from one generic initial condition.

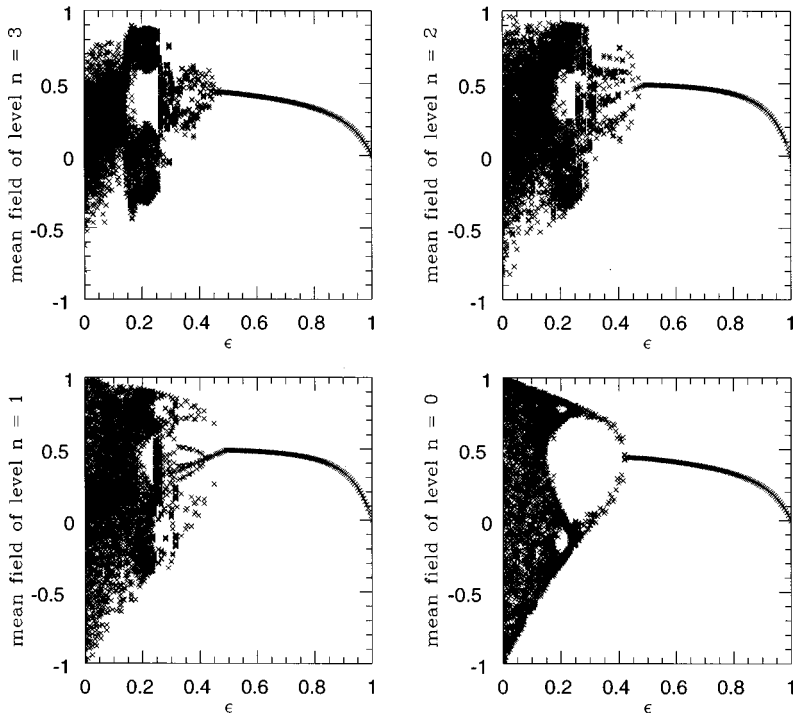

FIG. 2. Bifurcation diagrams for model II, in one dimension (with $L=3$), displaying the various dynamical phases, over the entire range of coupling strength: $0 \leqslant \epsilon \leqslant 1$. All four levels in the hierarchy ($n=0,1,2,3$) are depicted. These bifurcation diagrams are generated from one generic initial condition.

now giving the iterates of many superposed attractors.

Also, note that dimensionality does not play an important role in this system; i.e., the bifurcation diagrams obtained for one and two dimensions are essentially the same. This is quite expected, as dimensionality, as mentioned before, merely changes the sizes of the clusters of maps driving each other through their mean fields, in our hierarchical array of map ensembles.

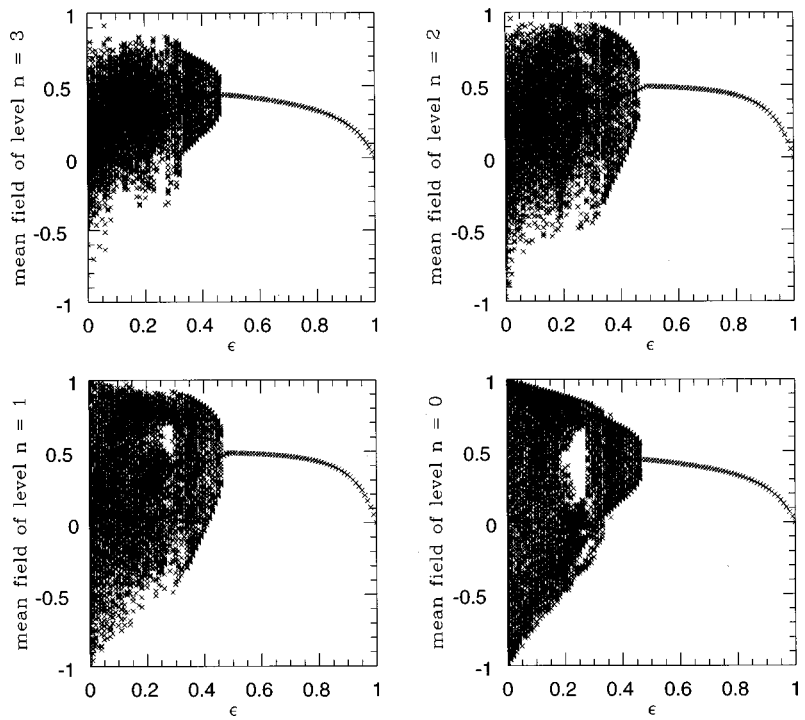

FIG. 3. Bifurcation diagrams for model I, in one dimension (with $L=3$), displaying the various dynamical phases, over the entire range of coupling strength: $0 \leqslant \epsilon \leqslant 1$. All four levels in the hierarchy ($n=0,1,2,3$) are depicted. These bifurcation diagrams are generated from a sample of 25 random initial phase points.

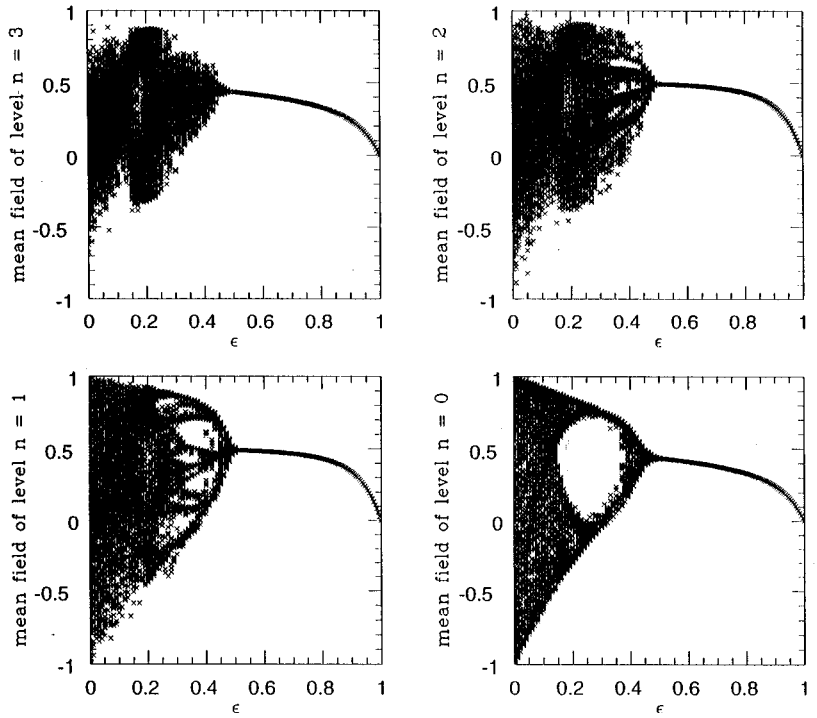

FIG. 4. Bifurcation diagrams for model II, in one dimension (with $L=3$), displaying the various dynamical phases, over the entire range of coupling strength: $0 \leqslant \epsilon \leqslant 1$. All four levels in the hierarchy ($n=0,1,2,3$) are depicted. These bifurcation diagrams are generated from a sample of 25 random initial phase points.

We now give details of the dynamical phases below.

B. Strong coupling phase ($0.5<\epsilon \leqslant 1.0$)

For both models I and II, when ϵ is reasonably high ($0.5<\epsilon \leqslant 1.0$) we find that the system goes to a spatially homogeneous state (at each level in the hierarchy), that is, it is synchronous at all levels. Furthermore, temporally the system dynamics goes to a *fixed point*. We give some features of the spectrum of steady state values below:

First, note that (a) $x^n_{\rm fixed}$ for model I is identical to that for model II, and (b) dimensionality does not affect the values of $x^n_{\rm fixed}$, as long as L remains the same (see Appendix for analysis). Figure 5 shows the steady state values of the various levels of the hierarchy, $x^n_{\rm fixed}$ versus level index n ($n=0,1,\ldots L$, $L=7$) for 4 values of ϵ: $\epsilon=0.9,0.8,0.7,0.6$. It is evident that there is a symmetry in the fixed point values of x^n with respect to hierarchy level n, namely, $x^n_{\rm fixed}=x^{L-n}_{\rm fixed}$. This is a result of the symmetry in the boundary conditions, namely, $h_{n-1}=0$ for $n=0$, and $h_{n+1}=0$ for $n=L$, which makes the form of the evolution equations [Eq. (4) for model I and Eq. (7) for model II] equivalent for the extrema levels, $n=0$ and L. Further, it is clear that the fixed point values are bounded between 0 and 0.5 for all values of ϵ. In the limiting case of $\epsilon=1.0$ the entire system evolves to $x^n_\tau=0$ for all τ and n (see Appendix).

The above scenario is very different from that encountered earlier in globally coupled maps on regular lattices. In the previous models one obtained synchronous states (that were spatially homogeneous) but evolving *chaotically* in time. Here we obtain synchronous states at each level of the hierarchy where every element becomes *temporally invariant* as well. Now the problem of ''controlling'' extended chaotic systems, which is currently evoking considerable interest [17], is essentially a search for systems (algorithms) that yield stable synchronized states. So our models above have immediate relevance to this problem as it enables the stabilization of large systems, not only spatially (as in previous examples) but also temporally. So the emergence of synchronized fixed point dynamics from the space-time hierarchical global coupling of chaotic elements may have practical utility in the control of macroscopically cascaded dynamical systems.

C. Moderate coupling phase ($0.15 \leqslant \epsilon \leqslant 0.5$)

For both models (I and II), the region of moderate coupling in parameter space, $0.15 \leqslant \epsilon < 0.5$, is marked by spatial inhomogeneity and temporal regularity. (The $\epsilon=0.5$ is a borderline system, i.e., the stability of the fixed point state is marginal here, and so its approach to steady state values is characterized by very long transience.)

Figure 6 displays a representative example for model II (in one dimension) with $L=3$, in the range $0.2 \leqslant \epsilon \leqslant 0.3$. (The diagram again shows the attractor obtained from the evolution of a single phase point.) Here the system is asynchronous, thus spatially inhomogeneous. But temporally it is evident from the bifurcation diagrams that large portions of the coupling parameter space support low order cycles of periodicity 2^k, $k=1,2,\ldots$. The regions not supporting exact cycles support noisy bands. The power spectrum of the noisy bands is characterized by prominent δ spikes at $f=2^{-k}$ on a broad background of noise. This feature can be seen in Fig. 7, which displays the power spectra for the mean field of 4 levels ($n=6,5,4,3$) at $\epsilon=0.2$, for model II in two-dimensions with $L=6$. This behavior is reminiscent of ''pe-

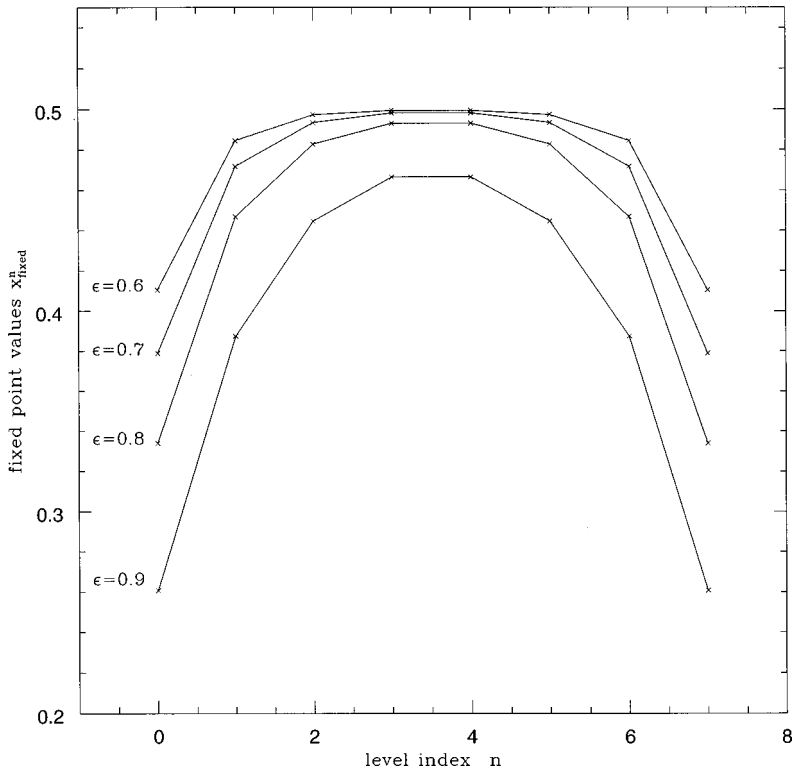

FIG. 5. Plot of fixed point values x^n_{fixed} vs level index n for models with $L=7$ and $\epsilon=0.6,0.7,0.8,0.9$.

riodic chaos'' in the logistic map where the iterates jump from one band to another in a periodic fashion (e.g., for the map $x_{n+1}=4rx_n(1-x_n)$ for $r=0.898\,143\ldots$ [18].)

Another very interesting feature is the manner in which an initial phase point jumps from attractor to attractor as ϵ is varied, as a result of the many coexisting attractors, with the initial phase point lying in different basins of attraction for different values of ϵ. This is most marked in the range $0.4 \leqslant \epsilon \leqslant 0.5$, and is discernable even for very high resolutions. See Figs. 8(a)–8(d) for successively enlarged portions of the

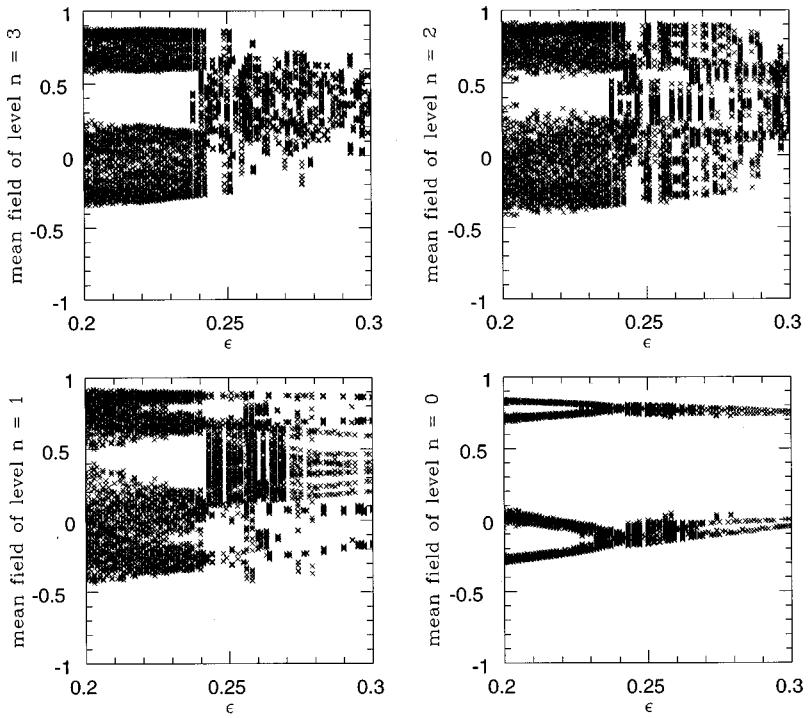

FIG. 6. Detailed section of the bifurcation diagrams for model II, in one dimension, with $L=3$, in the ranges $0.2 \leqslant \epsilon \leqslant 0.3$. All four levels in the hierarchy ($n=0,1,2,3$) are depicted. These bifurcation diagrams are generated from one generic initial condition.

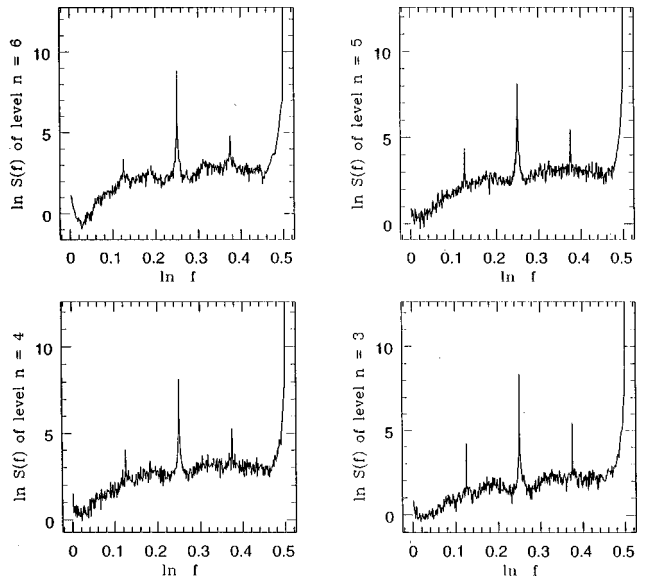

FIG. 7. Power spectrum of the mean field of the four hierarchical levels: $n=3,4,5,6$, for model II in two dimensions, with $L=6$, at $\epsilon=0.2$. Here we average over 20 runs of length 1024 each. The abscissa has frequency f and the ordinate has $\ln S(f)$ where $S(f)$ is the power.

ϵ space. Very clearly they look similar, and in this sense the *bifurcation diagram here is ''self-similar'' or ''fractal,'' reflecting fractal boundaries of the basins of attraction of the coexisting attractors*.

D. Weak coupling phase ($0 \leqslant \epsilon < 0.15$)

Now we operate in the region of parameter space where coupling is weak: $\epsilon < 0.15$. Here, for both models, there is no apparent synchronization, order, or correlation among the elements of the different levels of the hierarchy, in either space or time. However, one finds that rough periodicities emerge in the time evolution of the mean field of the levels, this effect being more pronounced at finer scales. Figures 9 and 10 show the power spectra of the mean field h^n at the finest hierarchy levels $n=6,5,4,3$ for models I and II in two dimensions, with number of levels $L=6$, at a representative values of ϵ. *It is clearly evident that the mean field develops collective beating patterns, which are manifested in prominent peaks in the power spectra*.

Another feature of this phase is that the mean field quantities may show many pronounced fine structures in their power spectrum, while the spectra of individual elements are broad and coarse. Figure 11 shows the spectrum of a single element for model I in two dimensions at hierarchy levels $n=6,5,4,3$ ($L=6$, $\epsilon=0.075$). Compare this to Fig. 10, which shows the spectrum of the mean field for the same levels. It seems clear then that for the finer levels (which have large number of elements) *the global quantity displays marked periodic structure while the individual element reflects only a coarse ''ghost'' of those periodicities*. These broad peaks are strongly reminiscent of the enormous collective beating *vis a vis* ''chaotic'' individual evolutions, seen in globally coupled maps on very large regular lattices. For the grosser levels (which have fewer elements), however, the evolution of the mean field simply reflects the evolution of the single element, very much like the situation for global coupling on small regular lattices.

Further, we investigate the statistical properties of the fluctuations of the mean field for the two models in this phase, hoping to uncover signatures of the subtle correlations among the levels in the hierarchy. Figures 12(a), 12(b), 13(a), and 13(b) give the mean square deviation (MSD) (for models I and II, in one and two dimensions, respectively) with respect to the number of elements N for the $L+1$ levels of the hierarchy, in the representative example of $\epsilon=0.07$. [In one dimension the system has number of levels $L=12$, and in two dimensions it has $L=7$. Note that $N=(2^n)^d$, $n=0,1,\ldots L$. So N spans the range 1 to 4096 for the 1D case and spans the range 1 to 16 384 for the 2D case.] *It is clearly apparent that the MSD does not decrease in a statistical fashion* (*i.e., as* $1/N$). *Instead it oscillates around a saturation value.* This signals the emergence of some subtle correlation among the chaotic elements at various levels in the hierarchy.

Note that globally coupled maps on regular lattices showed this kind of ''breakdown of the law of large numbers'' [1–9]. On the other hand local coupling on a hierarchical Cayley tree [15] displayed clear $1/N$ statistical decay of the deviations of the mean field with respect to number of sites on the tree. Also note that intrinsic fluctuations decay statistically in coupled map lattices with local and random nonlocal connections of finite connectivity [19]. This indicates that the nonstatistical features of the mean field dynamics that emerge in our models must arise from the effects of *global coupling*, which induces certain size independent remnant fluctuations [1–9].

IV. SUMMARY

In summary, we have constructed prototype models of globally coupled systems on lattices with space-time hierarchy. In our models fully chaotic dynamical elements at a certain level in the hierarchy are coupled to the levels immediately above and below in the hierarchy through their mean fields. We report the wealth of spatiotemporal phenomena our models yield and give detailed bifurcation diagrams in coupling parameter, ϵ, space ($0 \leqslant \epsilon \leqslant 1$). Importantly (especially in the context of control) we find that over a large range of reasonably high coupling ($0.5 < \epsilon \leqslant 1$) our models quickly evolve to a spatially homogeneous (synchronous) state where the dynamics is a fixed point, i.e., every element is temporally invariant. For moderate coupling $0.15 < \epsilon < 0.5$, we have spatial inhomogeneity (that is asynchronous evolution) and temporal regularity, marked by the presence of, either exact 2^k, $k=1,2\ldots$ cycles, or noisy bands (characterized by delta spikes on a noisy background in the power spectra). An interesting feature of this phase is the presence of several coexisting attractors, with fractal basin boundaries. For small coupling ($\epsilon \sim 0.1$) our system, while temporally chaotic and spatially nonhomogeneous, develops certain broad periodicities in their mean field, especially at finer scales. In addition, if one looks at the fluctuation of the mean field at various levels in the hierarchy in this phase, one finds that the mean square deviation does not decrease as $1/N$ with

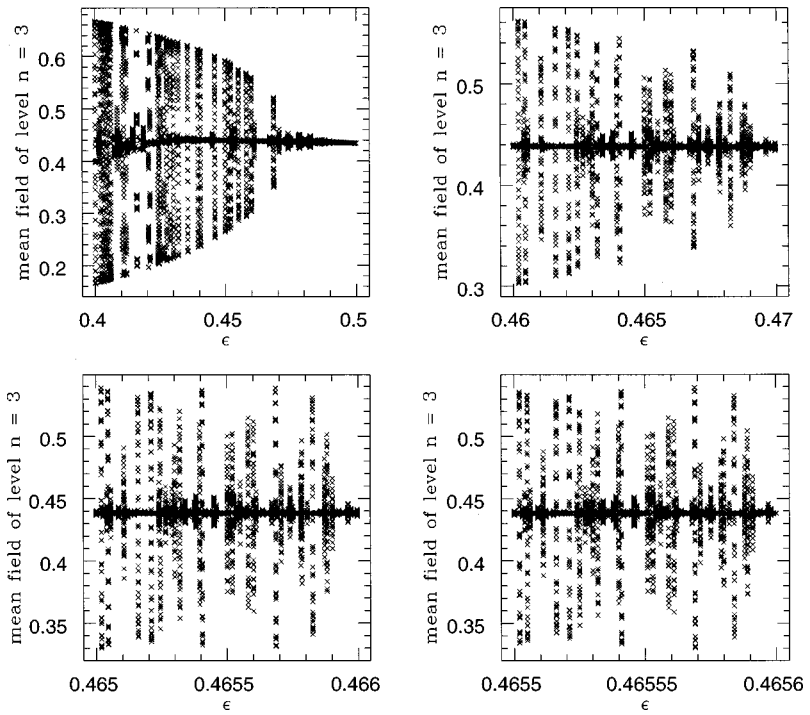

FIG. 8. Detailed sections of the bifurcation diagrams for model I, in one dimension, with $L=3$, in the ranges (a) $0.4\leqslant\epsilon\leqslant0.5$; (b) $0.46\leqslant\epsilon\leqslant0.47$; (c) $0.465\leqslant\epsilon\leqslant0.466$, and (d) $0.4655\leqslant\epsilon\leqslant0.4656$. Only level $n=3$ in the hierarchy is depicted. These bifurcation diagrams are generated from one generic initial condition.

N, where N is the number of elements at a particular level. Instead it displays marked nonstatistical behavior with the deviations saturating (or even increasing) for high N, indicating subtle collective correlations.

ACKNOWLEDGMENTS

G.P. and S.S. would like to thank the International Center of Theoretical Physics, Trieste, where this work was initiated, for its hospitality. Further, S.S. gratefully acknowledges the many very stimulating discussions on hierarchical lattices with Stefan Thomae, and G.P. acknowledges support from CONACyT (Mexico) through Grant No. 4178-E9405.

APPENDIX

Here we discuss static and dynamic features of synchronised (homogeneous) solutions.

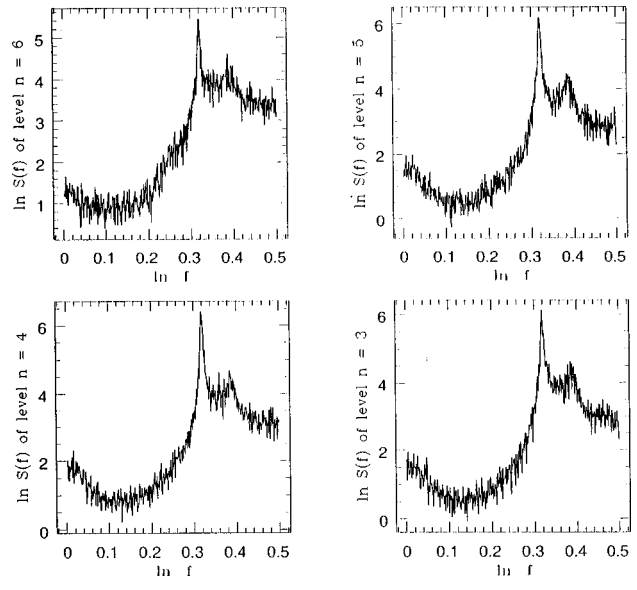

FIG. 9. Power spectrum of the mean field of model I in two dimensions with $L=6$, for the levels $n=6,5,4,3$ at $\epsilon=0.075$. Here we average over 20 runs of length 1024 each. The abscissa has frequency f and the ordinate has $\ln S(f)$ where $S(f)$ is the power.

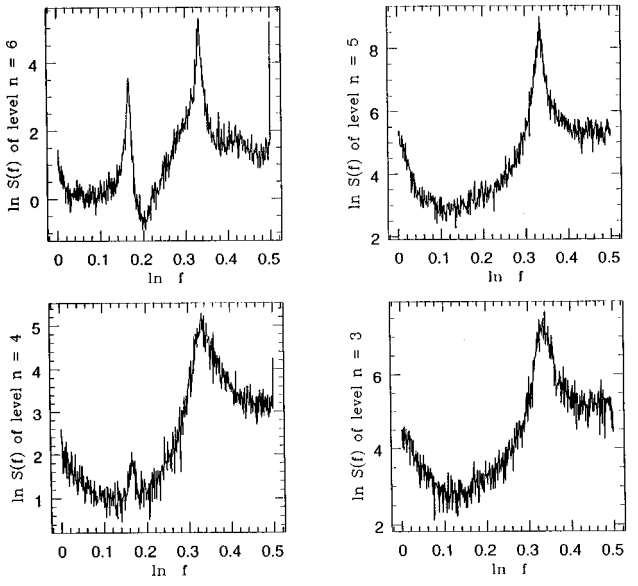

FIG. 10. Power spectrum of the mean field of model II in two dimensions with $L=6$, for the levels $n=6,5,4,3$ at $\epsilon=0.07$. Here we average over 20 runs of length 1024 each. The abscissa has frequency f and the ordinate has $\ln S(f)$ where $S(f)$ is the power.

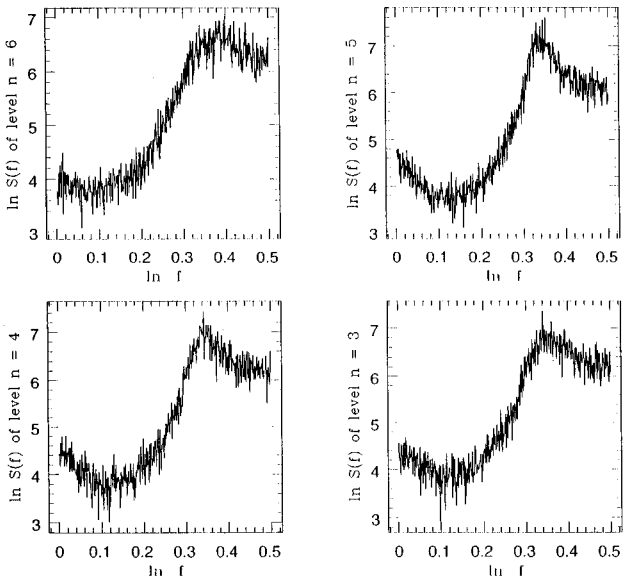

FIG. 11. Power spectrum of a single element at level $n=6,5,4,3$, for model I in two dimensions with $L=6$, at $\epsilon=0.075$. Here we average over 20 runs of length 1024 each. The abscissa has frequency f and the ordinate has $\ln S(f)$, where $S(f)$ is the power.

Static solution

First we briefly analyze the steady state properties of the various levels of the hierarchy in models I and II. Let us denote the fixed point values of the levels by $x^n_{\rm fixed}$ where n is the level index. Since the steady state conditions are spatially homogeneous we can drop the space index $\mathbf{r}$. Further, this implies that $h^n \equiv x^n_{\rm fixed}$. So the static solutions for both model I and model II satisfy the same condition:

$$x^n_{\rm fixed}=(1-\epsilon)f(x^n_{\rm fixed})+\frac{\epsilon}{2}(x^{n+1}_{\rm fixed}+x^{n-1}_{\rm fixed}), \qquad \text{(A1)}$$

where

$$f(x)=1-2x^2$$

satisfying the boundary conditions for $n=0$ and $n=L$. Also note here that the steady state condition, namely, Eq. (11), is identical for all dimensionalities as the coupling is global and the synchronicity condition allows us to replace the mean field by $x^n_{\rm fixed}$ at level n, as mentioned before. So the *only parameters affecting the spectrum of steady state values are* (a) the coupling strength ϵ, (b) the number of levels in the hierarchy, determined by L. It is obvious that $\epsilon=1$ gives $x^n_{\rm fixed}=x^{n+1}_{\rm fixed}=x^{n-1}_{\rm fixed}$ as a solution, with boundary condition $h^{n-1}=0$ for $n=0$ and $h^{n+1}=0$ for $n=L$. Thus the steady state for $\epsilon=1$ is $x^n_{\rm fixed}=0$ for all $n=0,1\cdots L$.

For fixed point values of $\epsilon\neq 1$ one has to numerically solve $L+1$ coupled nonlinear equations. We have checked to see that the solutions thus obtained are consistent with the values of $x^n_{\rm fixed}$, at various values of ϵ, obtained via numerical simulations.

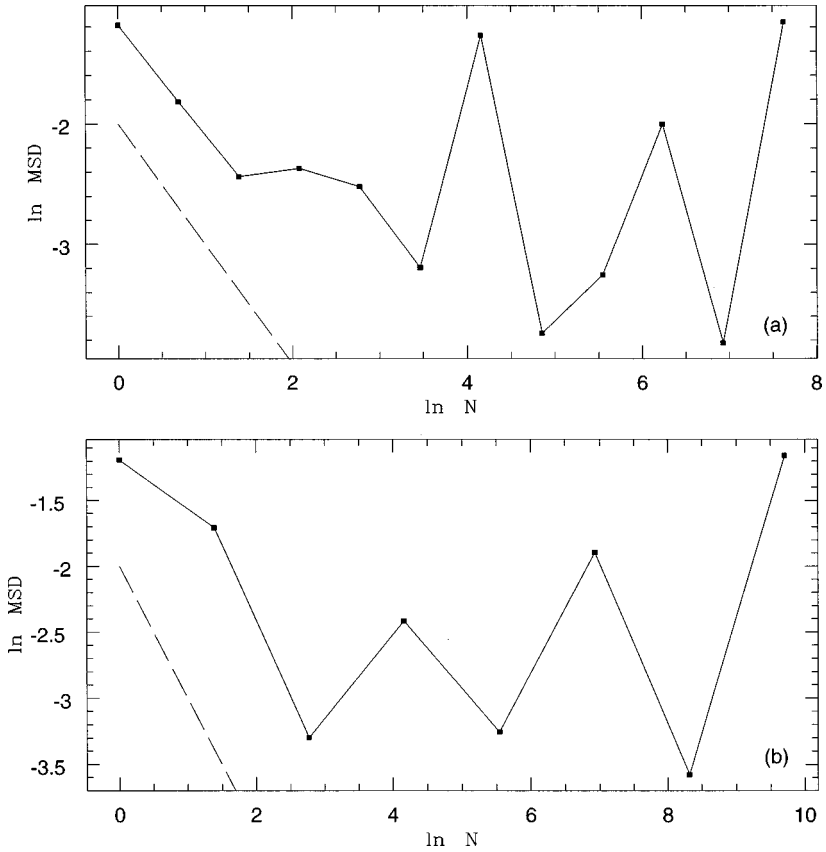

FIG. 12. Mean square deviation (MSD) of the mean field at a certain hierarchy level vs number of elements N at that level ($N=(2^n)^d$, where level index $n=0,1,\ldots,L$ and d is the dimension) for model I at $\epsilon=0.07$ in (a) one dimension, with $L=12$ (N spans the range 1 to 4096); and (b) two dimensions, with $L=7$ (N spans the range 1 to 16 384). The dotted line gives the $1/N$ statistical prediction.

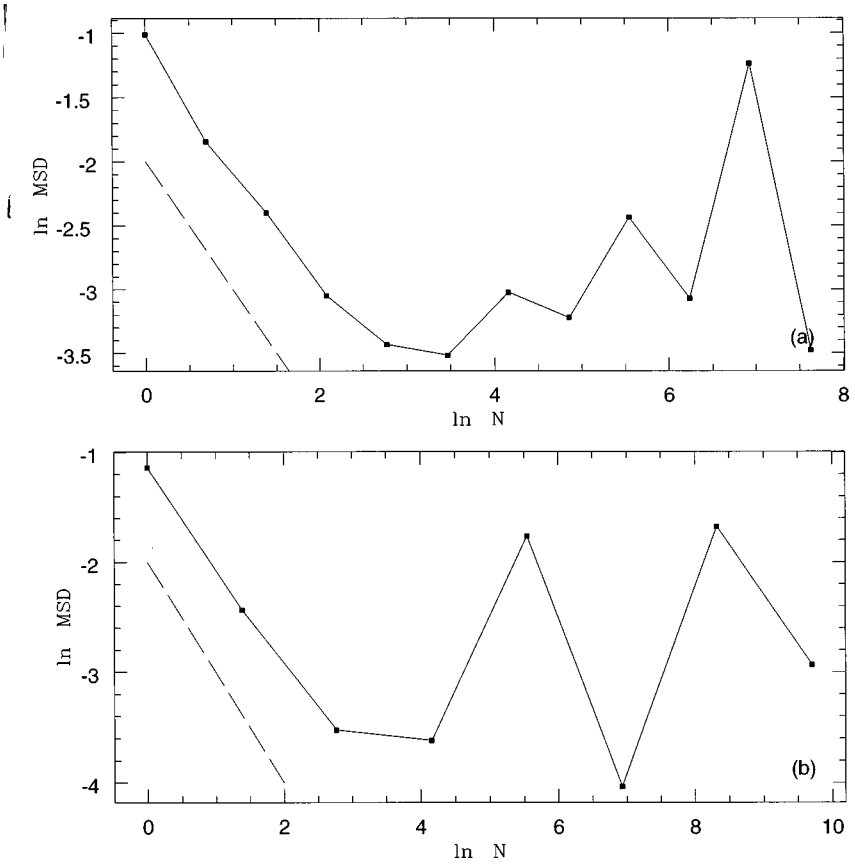

FIG. 13. Mean square deviation (MSD) of the mean field at a certain hierarchy level vs number of elements N at that level [$N=(2^n)^d$, where level index $n=0,1,\ldots,L$ and d is the dimension] for model II at $\epsilon=0.07$ in (a) one dimension, with $L=12$ (N spans the range 1 to 4096); and (b) two dimensions, with $L=7$ (N spans the range 1 to 163 384). The dotted line gives the $1/N$ statistical prediction.

Linear stability of the static solution

Now we investigate the linear stability of the static solution considering the dynamics of a small perturbation $\{\delta x^0,\delta x^1,\ldots,\delta x^L\}$. Note that we consider asynchronous (level-by-level) updates here. So a small perturbation at a certain level will affect its neighboring level only if its level index is higher. This yields (for both models)

$$x^n_{\text{fixed}}+\delta x^n_{\tau+1}=(1-\epsilon)\{1-2(x^n_{\text{fixed}}+\delta x^n_\tau)^2\}$$

$$+\frac{\epsilon}{2}(x^{n+1}_{\text{fixed}}+\delta x^{n+1}_\tau).$$

Canceling the zeroth-order terms on both sides and retaining only first-order terms in δx we find, using Eq. (4) and the upper line of Eq. (7),

$$\delta x^n_{\tau+1}=(1-\epsilon)(-4x^n_{\text{fixed}})\,\delta x^n_\tau+\frac{\epsilon}{2}\delta x^{n+1}_\tau. \qquad \text{(A2)}$$

The transfer matrix connecting the perturbation vectors at successive times is a $(L+1)\times(L+1)$ bidiagonal matrix, with diagonal entries

$$a_{ii}=-4(1-\epsilon)x^i_{\text{fixed}}$$

and off-diagonal entries

$$a_{ij}=\frac{\epsilon}{2}$$

when $j=i+1$. The absolute values of the of $L+1$ eigenvalues of the above matrix are $|\lambda^i_*|$, $i=1,2\cdots L+1$. Now $|\lambda^i_*|<1$ indicates stability, and $|\lambda^i_*|>1$ indicates linear instability of the ith eigenmode. Negative eigenvalues mean that the corresponding mode oscillates while positive values indicate monotonic behavior.

Now the eigenvalues of a bidiagonal matrix are equal to its diagonal elements, and so we have $\lambda^i_*=-4(1-\epsilon)x^i_{\text{fixed}}$. Utilizing the fact that $x^i_{\text{fixed}}<0.5$, for $\epsilon>0.5$, and $x^i_{\text{fixed}}=0.5$ at $\epsilon=0.5$, we easily obtain $\epsilon=0.5$ as the bifurcation point, and $0.5<\epsilon\leqslant 1$ as the stable regime of the spatiotemporal fixed point.

This analytical conclusion agrees completely with the numerical observations via simulations.

Synchronous updating algorithm

If one computed the mean field synchronously, one would obtain a different bifurcation diagram. Figure 14 shows one typical case for comparison. In the figure we have plotted the iterates at various hierarchy levels for model I in one dimension. Comparing with the corresponding case evolved via asynchronous rules (Fig. 1), it is clear that the real difference lies in the high ϵ range ($0.5\leqslant\epsilon\leqslant 1.0$), in particular in the stability properties of the fixed point regime [20]. *It is evi-*

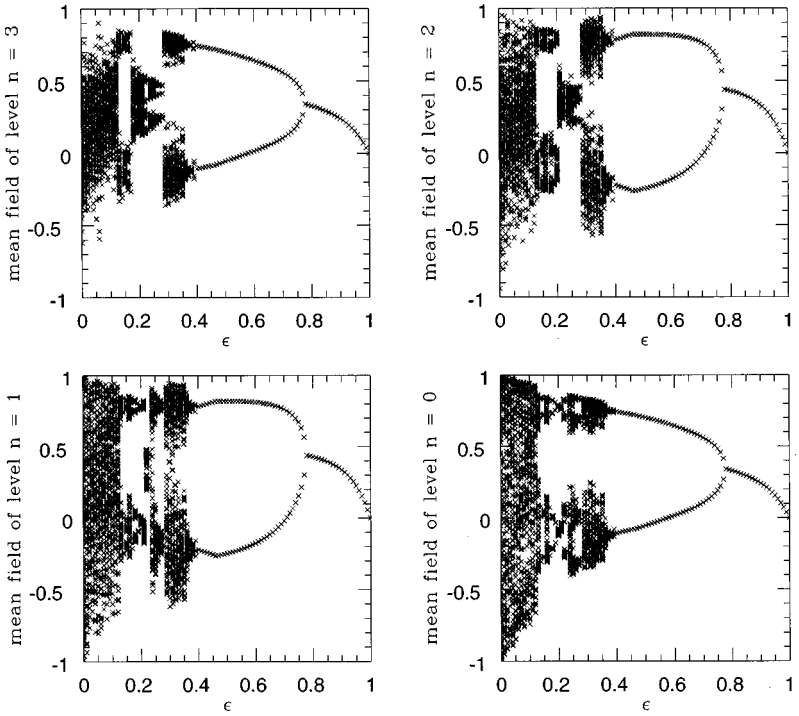

FIG. 14. Bifurcation diagrams for model I with synchronous updating rules ($L=3$) in one dimension, over the entire range of coupling strength: $0 \leqslant \epsilon \leqslant 1$. All the four levels in the hierarchy ($n=0,1,2,3$) are depicted. These bifurcation diagrams are generated from one generic initial condition.

dent that asynchronous updating allows the spatiotemporal fixed point to retain stability for a larger range of coupling strength, as compared with synchronous updating.

To account for this feature, we will briefly analyze here the linear stability of the spatiotemporal fixed point for the case of synchronous updating rules. Consider again the dynamics of a small perturbation $\{\delta x^0, \delta x^1, \ldots, \delta x^L\}$. Since the dynamics is now synchronous, perturbations at every level will influence *both* their neighboring levels. This yields (for both models)

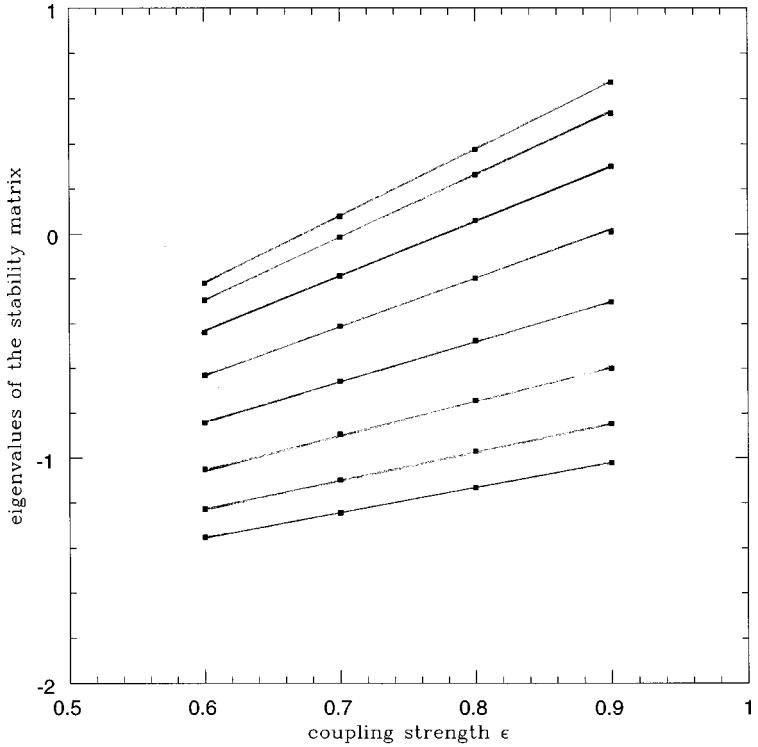

FIG. 15. Spectrum of eigenvalues of the stability matrix for different values of ϵ, for a system with $L=7$, evolving under synchronous updating rules.

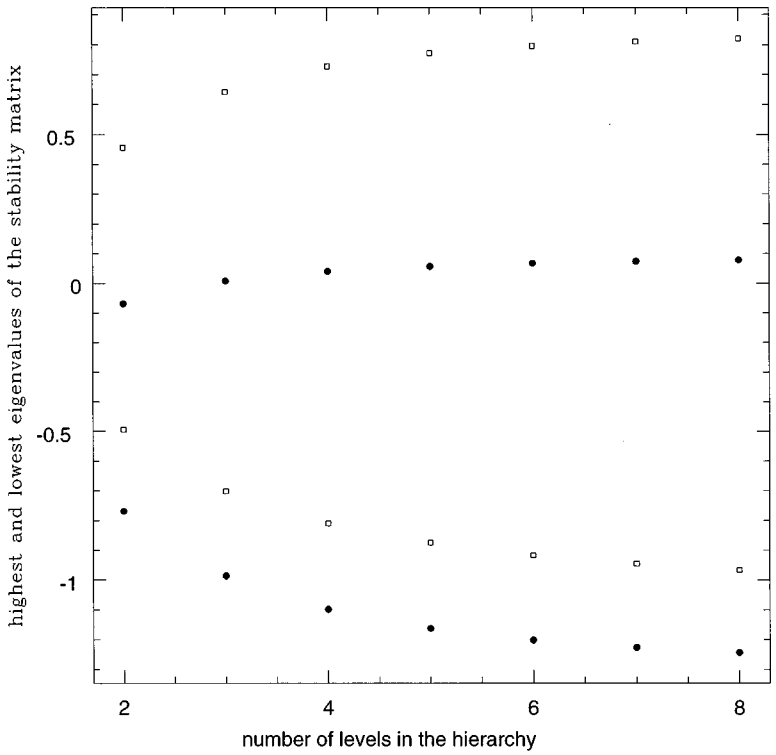

FIG. 16. The highest and lowest eigenvalues of the stability matrix for systems evolving under synchronous updating rules, with different number of hierarchical levels: $L=2,3,\ldots,8$, at two values of coupling strengths: $\epsilon=0.7$ (●), 0.95 (□).

$$x^n_{\text{fixed}}+\delta x^n_{\tau+1}=(1-\epsilon)\{1-2(x^n_{\text{fixed}}+\delta x^n_\tau)^2\}$$

$$+\frac{\epsilon}{2}(x^{n+1}_{\text{fixed}}+\delta x^{n+1}_\tau+x^{n-1}_{\text{fixed}}+\delta x^{n-1}_\tau).$$

Canceling the zeroth-order terms on both sides and retaining only first-order terms in δx we find, using Eq. (4) and the upper line of Eq. (7),

$$\delta x^n_{\tau+1}=(1-\epsilon)(-4x^n_{\text{fixed}})\,\delta x^n_\tau+\frac{\epsilon}{2}(\delta x^{n+1}_\tau+\delta x^{n-1}_\tau). \tag{A3}$$

The transfer matrix connecting the perturbation vectors at successive times is a $(L+1)\times(L+1)$ tridiagonal matrix, with diagonal entries

$$a_{ii}=-4(1-\epsilon)x^i_{\text{fixed}}$$

and off-diagonal entries

$$a_{ij}=\frac{\epsilon}{2}$$

when $i=j\pm1$. Again we have to study the absolute values of the of $L+1$ eigenvalues of the above matrix: $|\lambda^i_*|$, $i=1,2\cdots L+1$.

We can easily, numerically, find the eigenvalues of the above tridiagonal matrix. Figure 15 gives the spectrum of eigenvalues for different values of ϵ. Notice that the eigenvalues of the stability matrix increases linearly with ϵ. The bifurcation point (i.e., the ϵ at which $|\lambda^i_*|$ first exceeds 1, for some i) obtained by this analysis agrees very well with those obtained via simulations.

Figure 16 gives the highest and lowest eigenvalues for systems with different number of hierarchical levels L, for two values of coupling strength. It is clear that as L is increased the lowest and highest λ^i_* tend towards definite limits (for instance, for $\epsilon=0.7$, $\lambda_{\text{upper}}\sim0.08,\ldots$, $\lambda_{\text{lower}}\sim-1.26,\ldots$ and for $\epsilon=0.95$, $\lambda_{\text{upper}}\sim0.82,\ldots$, $\lambda_{\text{lower}}\sim-0.97,\ldots$). These values then give the upper and lower bounds for the eigenvalues of the system for a particular ϵ, when $L\to\infty$. The $L+1$ eigenvalues are clustered within these bounds. It is clearly evident that the bifurcation point ϵ_{bifur} is dependent on the number of levels in the hierarchy L, and tends to a limiting ϵ_{bifur} as $L\to\infty$ ($\epsilon_{\text{bifur}}\sim0.91,\ldots$). Note that this is unlike the asynchronous updating case where the bifurcation point is independent of L, with $\epsilon_{\text{bifur}}=0.5$. Comparing the ϵ_{bifur} obtained from the two kinds of updating rules, it is clear that asynchronous updating gives a much larger parameter region of stable spatiotemporal fixed points (and this is exactly what was observed in the numerics).

[1] K. Kaneko, Phys. Rev. Lett. **63**, 219 (1989); Physica D **41**, 38 (1990).
[2] K. Kaneko, Phys. Rev. Lett. **65**, 1391 (1990); Physica D **55**, 368 (1992).
[3] K. Kaneko, Physica D **54**, 5 (1991).
[4] G. Perez, C. Pando-L., S. Sinha, and H. A. Cerdeira, Phys. Rev. A **45**, 5469 (1992).
[5] G. Perez, S. Sinha, and H. A. Cerdeira, Physica D **63**, 341 (1993).
[6] G. Perez and H. A. Cerdeira, Phys. Rev. A **46**, 7492 (1992).
[7] S. Sinha, D. Biswas, M. Azam, and S. V. Lawande, Phys. Rev. A **46**, 3193 (1992).
[8] S. Sinha, D. Biswas, M. Azam, and S. V. Lawande, Phys. Rev. A **46**, 6242 (1992).
[9] D. Dominguez and H. A. Cerdeira, Phys. Rev. Lett. **71**, 3359 (1993).
[10] A. Crisanti, M. Falconi, and A. Vulpiani, Phys. Rev. Lett. **76**, 612 (1996).
[11] See, e.g., D. Amit, *Modelling Brain Function: The World of Attractor Neural Nets* (Cambridge University Press, Cambridge, 1989).
[12] R. Kopelman, Science **241**, 1620 (1988).
[13] D. L. Turcotte, *Fractals and Chaos in Geology and Geophysics* (Cambridge University Press, Cambridge, 1992).
[14] M. G. Cosenza and R. Kapral, Phys. Rev. A **46**, 1850 (1992).
[15] P. M. Gade, H. A. Cerdeira, and R. Ramaswamy, Phys. Rev. E **52**, 2478 (1995).
[16] It has been noticed in certain studies of spatially extended complex systems that synchronous and asynchronous updates give different universality classes of results, see for example: P. Marcq, H. Chate, and P. Manneville, Phys. Rev. Lett. **77**, 4003 (1996), which deals with different critical exponents arising in CML's evolving under synchronous and asynchronous rules; R. H. Swendsen and J.-S. Wang, Phys. Rev. Lett. **58**, 86 (1987), which deals with dynamical critical exponents in Monte Carlo simulations of equilibrium systems, involving different asynchronous updating schemes.
[17] Some references of this rapidly growing field of interest are: L. Pecora and T. M. Caroll, Phys. Rev. Lett. **64**, 821 (1990); Phys. Rev. A **44**, 2374 (1991); T. L. Caroll, Phys. Rev. E **50**, 2580 (1994); J. F. Heagy, T. L. Caroll, and L. M. Pecora, *ibid.* **50**, 1874 (1994); D. Auerbach, Phys. Rev. Lett. **72**, 1184 (1994).
[18] S. Thomae and S. Grossmann, J. Stat. Phys. **26**, 485 (1981).
[19] H. Chate and P. Manneville, Europhys. Lett. **17**, 291 (1992); Chaos **2**, 307 (1992).
[20] However, preliminary studies indicate that the emergent qualitative picture obtained from simulations via synchronous and asynchronous updating rules, in the low ϵ phase, is very similar.